Journal of Nuclear Materials 401 (2010) 149–153

Contents lists available at ScienceDirect

Journal of Nuclear Materials

journal homepage: www.elsevier.com/locate/jnucmat

Nanoindentation investigation of heavy ion irradiated $Ti_3(Si,Al)C_2$

X.M. Liu [a], M. Le Flem [a,*], J.L. Béchade [a], I. Monnet [b]

[a] CEA Saclay, DEN/DMN/SRMA/LA2M, 91191 Gif-Sur-Yvette Cedex, France
[b] Centre de recherche sur les Ions, les Matériaux et la Photonique, CEA/IRAMIS/CIMAP, 14076 Caen Cedex 5, France

ARTICLE INFO

Article history:
Received 12 November 2009
Accepted 14 April 2010

ABSTRACT

Because of good damage tolerance, thermal stability and interesting mechanical properties, Ti_3SiC_2, belonging to $M_{n+1}AX_n$ phases, has been considered as a potential candidate material for applications in the future Gas Fast nuclear Reactors (GFR) such as components of fuel cladding working between 500 °C and 800 °C. However, the outstanding mechanical properties of Ti_3SiC_2 related to a layered microstructure could be impacted by irradiation. In this work, high energy Kr and Xe ion irradiated $Ti_3Si_{0.95}Al_{0.05}C_2$ and $Ti_3Si_{0.90}Al_{0.10}C_2$ samples, provided by IMR Shenyang, Chinese Academy of Science, were characterized by nanoindentation technique. After irradiation at room temperature, an increase in hardness with irradiation dose was highlighted. Nevertheless, some damage tolerance remained because of preservation of the typical MAX layered structure. Irradiations at 300 °C and 500 °C lead to less significant increase suggesting irradiation defect annealing. A complete recovery of the properties at 800 °C seems to be obtained.

1. Introduction

The future Gas Fast nuclear Reactors (GFR) investigated in the scope of Generation IV forum [1] would operate at higher temperature and higher neutron flux (>0.1 MeV) compared to current nuclear systems. In-core components, such as fuel cladding, should be able to reach ambitious goals of dose (>100 dpa) and temperature (500–800 °C in nominal conditions and 1650 °C at least in accidental scenarios) [2]. These severe requirements are challenging in terms of materials: refractory metals such as W, Ta or Mo exhibit too large of an absorption cross-section and monolithic ceramics fail because of unacceptable brittleness leading to potential catastrophic failure. To increase toughness of ceramics, fibre reinforced matrix composites were considered and SiC_f/SiC [2,3] composites obviously turned out to be the best candidates to constitute fuel cladding in GFR.

In parallel, layered ternary compounds so-called MAX phases attracted attention to be used as a component of GFR cladding because they exhibit the benefit of both ceramics and metals. Indeed, these uncommon ceramics, $M_{n+1}AX_n$ (where $n = 1$, 2, or 3, M is an early transition metal, A is an A-group element, and X is either C or N [4]), have intrinsic damage tolerant properties linked to specific nanolayered structure of atomic planes allowing deformation via delamination and kink bands formation [5,6]. They also have high thermal conductivity [7] and excellent high temperature mechanical properties [8,9]. Among them, Ti_3SiC_2 [10] is promising because of its good thermal stability (between 1350 °C [11] and 1800 °C [12] depending on purity and atmosphere). This makes it potential candidate for GFR in-core applications, not as fuel element but rather as constituent of the GFR fuel cladding such as buffer or coating.

However, questionable points remain and the potentiality of Ti_3SiC_2 as constituent of GFR components must be demonstrated. Among the key points, the resistance of Ti_3SiC_2 toward neutron irradiation is of major interest. Indeed, possible microstructure evolution induced by irradiation may lead to change in mechanical properties; basically, embrittlement is observed in irradiated materials, even in low toughness ceramics [13]. This could be the main obstacle for the application of Ti_3SiC_2 as component in GFR. Consequently, both experimental neutron irradiations in French reactors and an irradiation program with charged particles on Ti_3SiC_2 compounds have been launched.

First investigations of microstructural changes after ion irradiation were reported, showing occurrence of lattice parameter change, disorder and potential amorphisation [14–16]. However, changes in mechanical properties of irradiated material had to be investigated. This study deals with ion irradiation induced hardness changes in $Ti_3(Si,Al)C_2$ compounds ($Ti_3Si_{0.95}Al_{0.05}C_2$ and $Ti_3Si_{0.90}Al_{0.10}C_2$), a solid solution of Ti_3SiC_2 and Al with improved purity and oxidation resistance. 74 MeV Kr and 92 MeV Xe ions were used to irradiate the materials at room temperature, 300 °C and 500 °C, from 1×10^{16} to 2×10^{19} ions m^{-2}. Nano-indentation measurements were performed on virgin and irradiated materials to

* Corresponding author. Address: CEA Saclay, DEN/DMN/SRMA, 91191 Gif-Sur-Yvette Cedex, France. Tel.: +33 (0)1 69 08 40 98; fax: +33 (0)1 69 08 71 30.
E-mail addresses: xmliu_9@hotmail.com (X.M. Liu), marion.leflem@cea.fr (M. Le Flem), jean-luc.bechade@cea.fr (J.L. Béchade), monnet@ganil.fr (I. Monnet).

0022-3115/$ - see front matter © 2010 Elsevier B.V. All rights reserved.
doi:10.1016/j.jnucmat.2010.04.015

obtain hardness evolution versus irradiation dose and temperature. Microstructural investigations were performed using scanning and transmission electron microscopy.

2. Experimental procedures

2.1. Material manufacture

The materials were fabricated by Institute of Metal Research, Chinese Academy of Sciences, Shenyang, China. It produced Ti_3SiC_2 with 5 at.% and 10 at.% of Al substituted for Si, i.e. $Ti_3Si_{0.95}Al_{0.05}C_2$ and $Ti_3Si_{0.90}Al_{0.10}C_2$: Al was shown to improve sample purity (no TiC secondary phase) and enhance oxidation resistance [17,18]. Detailed descriptions of the synthesis of Ti_3SiC_2 ceramics can be found elsewhere [17]. Briefly, the bulk $Ti_3(Si,Al)C_2$ ceramics were prepared by in situ hot pressing solid–liquid reaction of elemental powders. Ti, Si, Al, and graphite elemental powders (stoichiometric proportions) were mixed in a polyurethane mill for 20 h. The powder mixtures were then cold pressed in a graphite mould coated with a BN layer on the inner surface. The solid–liquid synthesis reaction and simultaneous densification were performed at about 1520 °C for 1 h, under a uniaxial pressure of 30 MPa (graphite the heating element, flowing argon atmosphere). The obtained materials exhibited high density and very few secondary phases (less than 3% in volume from X-ray diffraction analyses).

2.2. Irradiation experiments

The irradiation of the Ti_3SiC_2 ceramic was performed under high vacuum (10^{-6} torr) at Grand Accélérateur National d'Ions Lourds (GANIL) Caen, France. The ions were 74 MeV$^{+20}Kr^{86}$ (0.86 MeV/u) and 92 MeV$^{+23}Xe^{129}$ (0.71 MeV/u). The electronic stopping power of ions, the damage induced by nuclear interactions and the penetration depth of both ions were estimated by SRIM 2003 [19]. An example of penetration profile is shown in Fig. 1 for a dose of 1×10^{19} ions m^{-2}. For both ions, the maximum damage should be achieved between 7 and 8 μm to the surface dealing mainly with ballistic collisions and resulting ion implantation, while the first microns should be affected by electronic loss only (low damage level which decreases along the penetration depth). Optical observations on cross-section after irradiation confirmed SRIM predictions; an illustration of the damaged layer is given in Fig. 2.

For irradiations, $10 \times 5 \times 4$ mm^3 parallelepipedic samples were cut from $Ti_3Si_{0.95}Al_{0.05}C_2$ and $Ti_3Si_{0.90}Al_{0.10}C_2$. The large surface of each specimen was mechanically ground and polished down to 0.25 μm (diamond spray). The polished samples were decreased and washed with ethanol and acetone respectively.

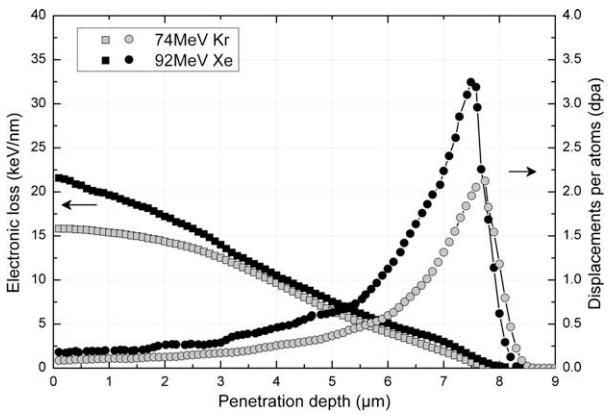

Fig. 1. Damage profile in Ti_3SiC_2 by 74 MeV Kr and 92 MeV Xe at dose of 1×10^{19} ions m^{-2} (SRIM simulation).

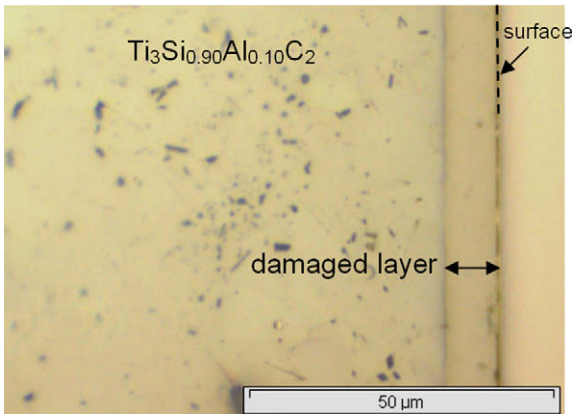

Fig. 2. Typical cross-section micrograph of $Ti_3(Si,Al)C_2$ after irradiation – here, $Ti_3Si_{0.90}Al_{0.10}C_2$ irradiated at room temperature with 72 MeV Kr (1×10^{19} ions m^{-2}).

The irradiation fluence levels ranged from 1×10^{16} to 2×10^{19} ions m^{-2} and irradiation surface was perpendicular to ion beam. The experiments were performed at room temperature, 300 °C and 500 °C.

For room temperature irradiations, to avoid temperature increase, flux was kept lower than 4.5×10^{12} ions m^{-2} s^{-1} for total fluence below 5.0×10^{17} ions m^{-2}. For high fluences (1×10^{18} ions m^{-2} and higher), flux of 4.5×10^{13} ions m^{-2} s^{-1} was selected to fit the beam time schedule: a sample stage with cooling water was used to avoid temperature increase during irradiation. In all cases, samples were directly pasted on the stage by electrically conductive double-side carbon adhesive discs and the temperature raise was lower than 40 °C.

For high temperature irradiations, a dedicated stage was used. Samples were fixed on the stage by a piece of stainless steel. The heating resistance and thermal couple were placed below the copper plate to make sure a rapid heating rate and accurate measurement/regulation of sample temperature. Cooling air was purged through a stainless steel tube welded on the back of copper stage after irradiation to ensure rapidly decrease of sample temperature.

After irradiation, examination of the surfaces and indentations was performed by scanning electron microscopy (SEM). Additional X-ray photoemission spectroscopy (XPS), energy dispersive spectroscopy (EDS) and wavelength dispersive X-ray spectroscopy (WDS) analyses showed the oxidation was limited to the first 10–100 nm at the surface except for samples irradiated with Xe at 500 °C where oxidation reached ~300 nm in depth: this oxide layer was removed by careful polishing with diamond paste (0.25 μm) until the sample turned shiny (the removed layer was estimated to ~500 nm).

Annealing of $Ti_3Si_{0.95}Al_{0.05}C_2$ irradiated with Kr at room temperature up to 1×10^{19} ions m^{-2} was performed in a tubular furnace with flowing argon at 340 °C, 430 °C, 500 °C and 800 °C (1 h). The hardness of the annealed sample was obtained by nanoindentation.

2.3. Nanoindentation

Nanoindentation technique has been established as the main tool for investigating the mechanical properties of small volumes of material especially the surface hardness of materials. This technique has been widely used when investigating the hardness change of materials after ion irradiation [20–23]. A Nano Instrument's nanoindenter^{XP} was adapted to examine the change of hardness and elastic modulus after irradiation. A Berkovich diamond indenter tip was used to perform the nano-indentation measurements on the surface of the irradiated samples. Before making indentation acquisition, an optical microscope attached on the

instrument was used to select satisfactory area (no scratches, no pull-out or secondary phases ...). The distance between microscope and indenter tip was calibrated before each indentation test to reduce position error of indentation. To eliminate the influence of the indentation size effect on final hardness value, measurements were performed using a constant depth method. Hardness was extracted from the unloading curves of each load and average hardness was deduced. Examinations both on cross-section and on the surface of irradiated bulk samples were performed.

It must be noted that irradiation profiles were not constant as a function of depth and the stress field from the indenter extends about seven times the contact depth [24]. Consequently, the measured hardness values as a function of depth did not represent the actual hardness of the material at that depth. Nevertheless, because the shape of the irradiation profile remains consistent for a given ion species and energy, it is reasonable to use the nanoindentation measurements to compare the relative effect of irradiation. Relative change in hardness has then been considered:

$$H_{\mathrm{irr}} = H_o \times (1 + \Delta\%)$$

where H_{irr} is the hardness after irradiation, H_o is the hardness before irradiation and $\Delta\%$ is the relative change in hardness induced by irradiation.

The Berkovich diamond indenter tip samples the hardness in the region of the indent and extends down about seven times the indenter's contact depth [24]. Thus, since the ion stopping ranges are about 8 μm, a constant penetration depth of 1100 nm (corresponding to a ~400 mN load) was applied to attempt to get hardness down to peak damage layer, without contribution from underneath non-irradiated bulk (the contribution from thin oxide layer at the surface of the sample could be neglected). About 20 indents were made at the surface, distance between two indents was at least 30 μm. Scanning electron microscope was used to observe indents at the surface of highly irradiated samples.

3. Results

Evolution of hardness with irradiation doses at room temperature is shown in Fig. 3 for $Ti_3Si_{0.90}Al_{0.10}C_2$ samples irradiated with both ions. It can be seen that, considering the test error, hardness change is not significant for samples irradiated up to fluences of 1×10^{16} and 1×10^{17} ions m^{-2}. With further increasing irradiation fluence, hardness increases linear until fluence of 1×10^{19} ions m^{-2} for both ions: for this dose the hardness is more than doubled. It is not so obvious whether there is a significant effect of the irradiating ion (from SRIM calculation Kr should induce less damage level than Xe, which may be perceptible from Fig. 3 but not so dramatic). Hardness of sample irradiated with Xe to 2×10^{19} ions m^{-2} is a little bit lower, at least not higher considering experiment error, than for the 1×10^{19} ions m^{-2} sample, which suggests a saturation effect. Besides, no effect of Al contents on hardness change could be observed for the two kinds of materials investigated, as shown in Fig. 4.

To estimate the influence of irradiation on damage tolerance properties of this compound, SEM examinations of indentations were performed on high irradiated specimens. Fig. 5a shows an indentation after Kr irradiation to 1×10^{19} ions m^{-2}, which is very similar to the indentation before irradiation: no crack could be induced at the corner of the indentation and typical slip band features of the nanolaminate structure of Ti_3SiC_2 are obvious (arrowed), corresponding to slip systems along basal planes [5]. Observations were also performed on specimens irradiated with Xe above 1×10^{19} m^{-2} (Fig. 5b) but detection of the slip bands was disturbed by surface layers formed on the sample during irradiation (white spots, so-called "hills" previously reported by [16]). However, no cracking emanates from the corners of the indent.

After irradiation at 300 °C and 500 °C, the hardness change with dose is much less significant as shown in Fig. 6. If no difference between room temperature and high temperature occurs for fluence level of 1×10^{16} and 1×10^{17} ions m^{-2}, the hardness at higher doses is obviously lower after irradiation at high temperature. For instance, for Kr irradiation to 1×10^{19} ions m^{-2}, the hardness relative increase is 115% at room temperature and reaches only 30% after irradiation at 500 °C. Same trends can be observed for Xe irradiation at 300 °C and 500 °C. Fig. 6b also highlights the effect of the oxide layer formed at 500 °C for fluence level of 1×10^{19} ions m^{-2} inducing low surface hardness (i.e. this oxide was obviously softer than $Ti_3(Si,Al)C_2$); the true hardness of the sample was recovered after removing the oxide layer by polishing, which lead to consistency with the expected trend.

According to these results, increasing irradiation temperature results in a lower hardness increase, which suggests irradiation defect annealing occurred at 300 °C and 500 °C. To more precisely measure the temperature where hardness begins to drop and the irradiation temperature to induce a complete recovery of defects, some primary annealing on the $Ti_3Si_{0.95}Al_{0.05}C_2$ sample irradiated with Kr to fluence of 1×10^{19} ions m^{-2} was performed. As shown in Fig. 7, the hardness starts to drop as early as 300 °C; at 800 °C

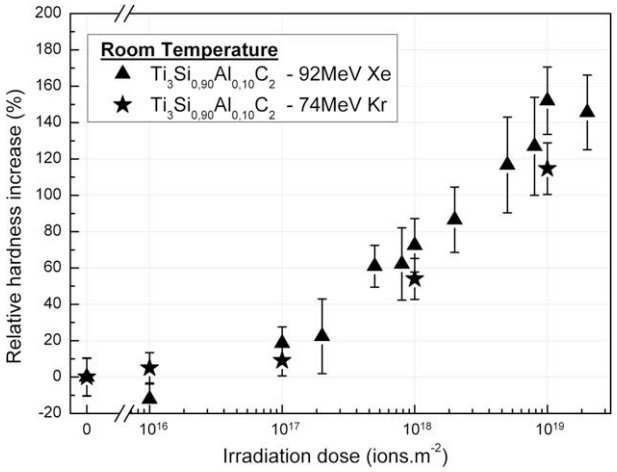

Fig. 3. Change in surface hardness of $Ti_3(Si,Al)C_2$ versus irradiation dose at room temperature – effect of irradiating particle.

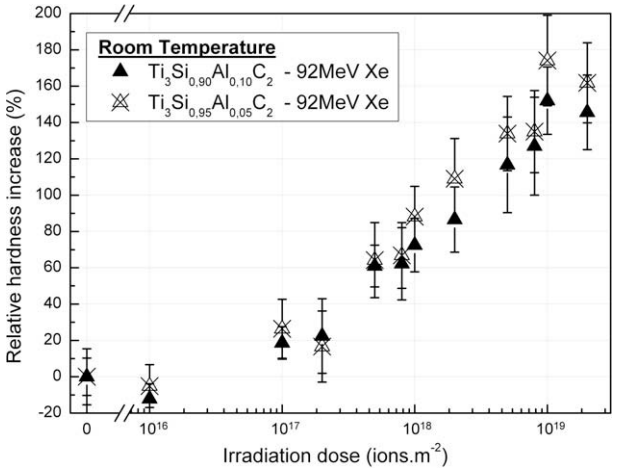

Fig. 4. Change in surface hardness of $Ti_3(Si,Al)C_2$ versus irradiation dose at room temperature – effect of Al content (92 MeV Xe).

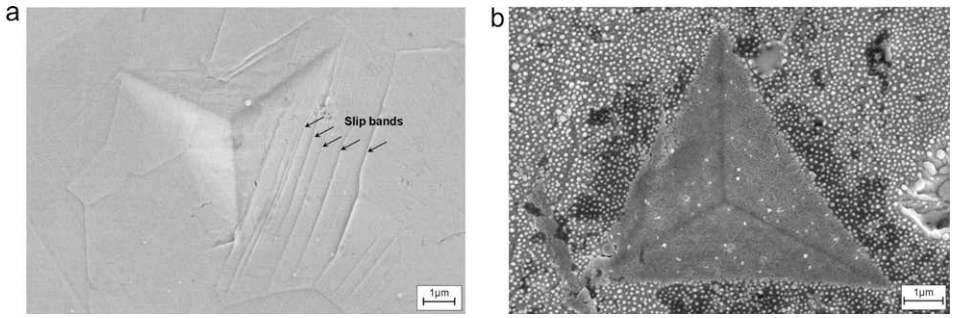

Fig. 5. SEM Morphology of indents on $Ti_3Si_{0.95}Al_{0.05}C_2$ irradiated (a) with 74 MeV Kr to 1×10^{19} ions m^{-2} and (b) with 92 MeV Xe to 2×10^{19} ions m^{-2}. White spots on (b) correspond to "hills" formation previously reported by [16].

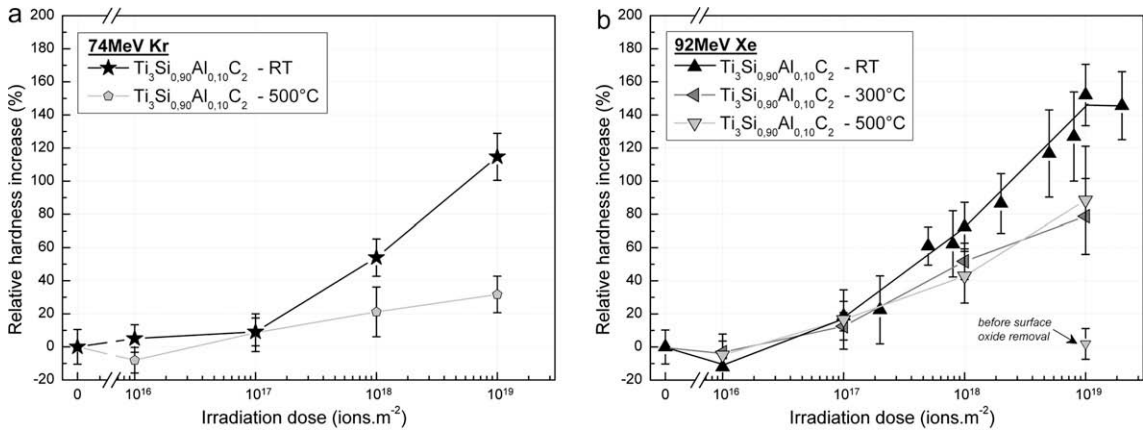

Fig. 6. Effect of high temperature irradiation on $Ti_3(Si,Al)C_2$ surface hardness (a) 74 MeV Kr and (b) 92 MeV Xe irradiations.

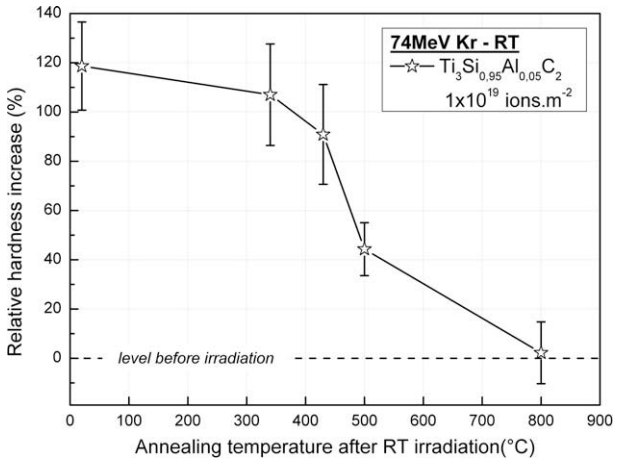

Fig. 7. Effect of post-irradiation annealing on the surface hardness of room temperature irradiated $Ti_3(Si,Al)C_2$ (irradiated up to 1×10^{19} Kr m^{-2}).

it is almost the same as the virgin sample value. It suggests that most of defects produced by irradiation have been recovered. This behaviour is promising for application above 500 °C i.e. in the range of operating temperature of GFRs.

4. Discussion

The strong dependence of $Ti_3(Si,Al)C_2$ hardness with irradiation dose and irradiation temperature could not be attributed to oxidation or dramatic chemical change at the surface of the sample. This must be directly related to formation of irradiation defects, as previously reported in other ceramics [26–28]. The present results are consistent with evolution of the microstructure during irradiation. While, X-ray diffraction analysis suggests occurrence of microstrains in ion irradiated $Ti_3(Si,Al)C_2$ [14], transmission electron microscopy suggested formation of black dots [15], i.e. clusters of point defects, acting as pinning centres for dislocations and interfere with planar gliding. Besides, these microstructural investigations did not allow to highlight any amorphisation of $Ti_3(Si,Al)C_2$ under irradiation: amorphisation is not suspected either from nanoindentation experiments since it would have lead to a drop in hardness (such as in SiC after irradiation at room temperature [23,29]) not observed in this work.

The progressive recovery of hardness with temperature (irradiation temperature or post-irradiation annealing) is explained in terms of recombination and annealing of point defects.

One basic interesting characteristic of Ti_3SiC_2 is its damage tolerance property. Vickers indentations in brittle solids basically result in sharp cracks extending from corners of the indents meaning low toughness. Instead of crack formation, delaminations, kinking of individual grains, grain push-outs and pull-outs are basically observed in the area around indentations in Ti_3SiC_2 [25]. SEM examination of indentations in $Ti_3(Si,Al)C_2$ irradiated up to 1×10^{19} m^{-2} and 2×10^{19} m^{-2} showed no cracks could be induced (Fig. 5) suggesting the material is still damage tolerant despite strong increase in hardness. However, this preservation of tolerance property may be controversial. It is the case for irradiated SiC where an apparent increase in toughness is basically observed from indentation analysis but may be interpreted as an increase in cleavage resistance brought by irradiation [30]. In ion irradiated specimens, affected

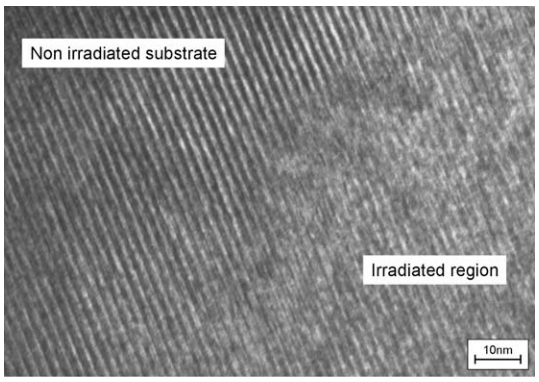

Fig. 8. High resolution transmission electron microscopy imaging of ion implanted region in $Ti_3Si_{0.90}Al_{0.10}C_2$ irradiated with 92 MeV Xe to 7.5×10^{18} ions m^{-2}. Despite atomic disorder induced by irradiation, the typical layered structure of Ti_3SiC_2 is obvious in both irradiated and non-irradiated areas.

within a thin layer, the heterogeneous swelling induced by point defects formation could also lead to compressive stress at the very surface making hazardous any interpretation [31]. However, cross-sectional exams of residual indentation impression in ion irradiated SiC showed micro-cracks formation allowing both fracture energy dissipation and toughening [32]. Thus, it sounds uneasy to draw from basic examination of indentations conclusions about irradiation effects on toughening. Nevertheless, presence of characteristic sliding features parallel to the print edge (arrowed in Fig. 5) means $Ti_3(Si,Al)C_2$ is still able to confine the damage, i.e. is still (to a certain extend) damage tolerant after dose of 1×10^{19} Kr m^{-2}. This can be attributed to preservation of the typical layered structure of Ti_3SiC_2 after irradiation suggested by High Resolution TEM analysis. Fig. 8. showing the implantation peak region for the 7.5×10^{18} ions m^{-2} specimen clearly shows that despite the perturbation of the staking in the irradiated area, the nanolaminate structure remains.

5. Conclusions

Nanoindentation investigation was performed on $Ti_3(Si,Al)C_2$ ceramics irradiated with high energy ions, 74 MeV Kr and 92 MeV Xe. Evaluation of hardness with irradiation dose, irradiation temperature, irradiating particles and Al content in samples was studied. The following conclusions could be drawn from this investigation.

- Ions penetration depth determined by SRIM simulation and cross-section exams showed the damage layer was ~8 μm in thickness.
- Xe and Kr ions induced the same effects on hardness evolution, and almost in the same proportion (a slightly larger increase was observed when using Xe ions).
- After room temperature experiment, limited increase in hardness was detected below 1×10^{17} ions m^{-2}. Above, significant increase with increasing irradiation dose was obvious, which must be linked to increases in point defects densities. At 1×10^{19} ions m^{-2}, the hardness was at least doubled. A saturation is suggested for higher doses.
- Irradiation at 300 °C and 500 °C induced a less pronounced increase in hardness meaning recovery of properties which is to be related to irradiation defects annealing. This was confirmed by post-irradiation heat treatments suggesting the defect annealing would be almost total at 800 °C according to hardness evolution.
- Al content (5 at.% or 10 at.%) did not seem to have a significant effect on hardness or change in hardness with irradiation.
- In the range of investigated irradiation dose, damage tolerance ability of $Ti_3(Si,Al)C_2$ seemed to be preserved.

According to the present work showing damage tolerance preservation after irradiation at room temperature and limited increase in hardness above 500 °C, it can be concluded that Ti_3SiC_2 and related compounds could be promising materials for use in future GFRs.

Acknowledgements

Authors are very grateful to Professor Yanchun Zhou from Institute of Metal Research, Chinese Academy of Sciences, Shenyang, China, for having providing the samples: he is thanked for collaborative work and fruitful discussions. Authors would like to thank Mr. Pierre Forget for his help with nano-indentation experiments, Mr. Patrick Bonnaillie who performed FEG-SEM examinations and Mrs. S. Doriot and Mr. Theodore Cozzika for TEM imaging. All of them belong to the Nuclear Material Department at CEA Saclay.

References

[1] A Technology Roadmap for Generation IV Nuclear Energy Systems, The US DOE Nuclear Energy Research Advisory Committee and the Generation IV International Forum, 2002.
[2] P. Yvon, F. Carré, J. Nucl. Mater. 385 (2009) 217–222.
[3] Gas-Cooled nuclear Reactors/A Monography of the Nuclear Energy Directorate, Commissariat à l'Energie atomique, CEA Saclay and Groupe Moniteur: Editions du Moniteur, Paris, 2006.
[4] M.W. Barsoum, Prog. Solid State Chem. 28 (2000) 201–281.
[5] M.W. Barsoum, L. Farber, T. El-Raghy, Metall. Mater. Trans. A 30 (1999) 1727–1738.
[6] Y.W. Bao, C.F. Hu, Y.C. Zhou, Mater. Sci. Technol. 22 (2006) 227–230.
[7] M.W. Barsoum, T. El-Raghy, C.J. Rawn, W.D. Porter, H. Wang, E.A. Payzant, C.R. Hubbard, J. Phys. Chem. Solids 60 (1999) 429–439.
[8] M. Radovic, M.W. Barsoum, T. El-Raghy, J. Seidensticker, S. Wiederhorn, Acta Mater. 48 (2000) 453–459.
[9] C.J. Gilbert, D.R. Bloyer, M.W. Barsoum, T. El-Raghy, A.P. Tomsia, R.O. Ritchie, Scripta Mater. 238 (2000) 761–767.
[10] M.W. Barsoum, T. El-Raghy, M. Radovic, Interceram 49 (2000) 226–233.
[11] C. Racault, F. Langlais, R. Naslain, J. Mater. Sci. 29 (1994) 3384–3392.
[12] R. Radakrishnan, J.J. Williams, M. Akinc, J. Alloys Compd. 285 (1999) 85–88.
[13] M.C. Osborne, J.C. Hay, L.L. Snead, D. Steiner, J. Am. Ceram. Soc. 82 (1999) 2490–2496.
[14] X.M. Liu, M. Le Flem, J.L. Béchade, F. Onimus, T. Cozzika, I. Monnet, Nucl. Instrum. Methods B 268 (2010) 506–512.
[15] M. Le Flem, X.M. Liu, S. Doriot, T. Cozzika, F. Onimus, J.L. Béchade, I. Monnet, Y.C. Zhou, $Ti_3(Si,Al)C_2$ for nuclear application: investigation of irradiation effects induced by charged particles, in: Proc. of the 33rd International Conference on Advanced Ceramics and Composites, January 18–23, 2009, Daytona Beach, USA.
[16] J.C. Nappé, J. Nucl. Mater. 385 (2009) 304–307.
[17] Y.C. Zhou, H.B. Zhang, M.Y. Liu, J.Y. Wang, Y.W. Bao, Mater. Res. Innovations 8 (2004) 97–102.
[18] H.B. Zhang, Y.C. Zhou, Y.W. Bao, M.S. Li, Acta Mater. 52 (2004) 3631–3637.
[19] F. Ziegler. <http://www.srim.org/>.
[20] J.D. Hunn, E.H. Lee, T.S. Byun, L.K. Mansur, J. Nucl. Mater. 282 (2000) 131–136.
[21] J.D. Hunn, E.H. Lee, T.S. Byun, L.K. Mansur, J. Nucl. Mater. 296 (2001) 203–209.
[22] P. Hosemann, J.G. Swadener, D. Kiener, G.S. Was, S.A. Maloy, N. Li, J. Nucl. Mater. 375 (2008) 133–143.
[23] X. Kerbiriou, J.M. Costantini, M. Sauzay, S. Sorieul, L. Thomé, J. Jagielski, J.J. Grob, J. Appl. Phys. 105 (2009) 073513.
[24] L.E. Samuels, T.O. Mulhearn, J. Mech. Phys. Solids 5 (1957) 125–134.
[25] T. El-Raghy, A. Zavaliangos, M.W. Barsoum, S. Kalidindi, J. Am. Ceram. Soc. 80 (1997) 513–516.
[26] H. Suematsu, H. Iseki, T. Yano, Y. Saito, T. Suzuki, T. Mori, J. Am. Ceram. Soc. 75 (1992) 1742.
[27] T. Iseki, M. Tezuka, C. Kim, T. Suzuki, H. Suematsu, T. Yano, J. Nucl. Sci. Technol. 30 (1993) 68.
[28] Y. Yang, C.A. Dickerson, H. Swoboda, B. Miller, T.R. Allen, J. Nucl. Mater. 378 (2008) 341–348.
[29] C.J. McHargue, J.M. Williams, Nucl. Instrum. Methods B 80–81 (1993) 889–894.
[30] Y. Katoh, L.L. Snead, J. ASTM Int. 2 (2005) 8.
[31] M. Ménard, M. Le Flem, L. Gélébart, I. Monnet, V. Basini, M. Boussuge, Irradiation effects on the microstructure and mechanical properties of silicon carbide, in: Proc. of the 31st International Conference on Advanced Ceramics and Composites, January 21–26, 2007, Daytona Beach, USA.
[32] K.H. Park, T. Hinoki, A. Kohyama, J. Nucl. Mater. 367–370 (2007) 703–707.